



Foam Cell-Derived CXCL14 Multi-Functionally Promotes Atherogenesis and Is a Potent Therapeutic Target in Atherosclerosis

Weilin Tong^{1,2} · Yaqi Duan^{1,2} · Rumeng Yang^{1,2} · Ying Wang^{1,2} · Changqing Peng^{1,2} · Zitian Huo^{1,2} · Guoping Wang^{1,2}

Received: 16 August 2019 / Accepted: 11 September 2019 / Published online: 14 November 2019
© Springer Science+Business Media, LLC, part of Springer Nature 2019

Abstract

CXC chemokine family has been related to atherogenesis for long. However, the relationship between CXCL14 and atherogenesis is still unclear. This study preliminarily detected CXCL14 expression at foam cells in atherosclerosis specimens by immunohistochemistry. In vitro foam cells were derived from THP-1 after phorbol-12-myristate-13-acetate (PMA) and oxidized low-density lipoprotein (ox-LDL) stimulation. Immunoblotting and qPCR convinced CXCL14 expression variation during foam cell formation. We further demonstrated that ox-LDL regulated CXCL14 expression by AP-1. AP-1 could bind to CXCL14 promoter and up-regulate CXCL14 mRNA expression. Besides, CXCL14 promoted THP-1 migration, macrophage lipid phagocytosis, and smooth muscle cell migration as well as proliferation mainly via the ERK1/2 pathway. Additionally, a CXCL14 peptide-induced immune therapy showed efficacy in ApoE^{-/-} mouse model. In conclusion, our study demonstrated that CXCL14 is highly up-regulated during foam cell formation and promotes atherogenesis in various ways. CXCL14 may be a potent therapeutic target for atherosclerosis.

Keywords Foam cell · Atherogenesis · CXCL14

Introduction

Atherosclerosis is a vasculature disease characterized by chronic inflammation in the walls of arteries [1]. Monocyte recruitment into subendothelial space of artery walls and formation of foam cell are the main characteristics of atherosclerosis [2]. The recruitment of immune cells is mainly

modulated by adhesion molecules and chemokines [3]. Among the CXC chemokine family, CXCL12/CXCR4 signal pathway has been related to the pathogenesis of atherosclerosis for long [4]. CXCL12/CXCR4 axis aggravates various inflammatory diseases, which are related to immune cell recruitment [5]. In atherosclerosis, CXCR4 expression has been reported to increase as a result of macrophage-colony-stimulating factor (M-CSF) and ox-LDL stimulation [6]. Recent evidence by Sophie Merkelbach et al. [7] further showed that CXCL12 and CXCR4 mRNA expression was significantly increased in carotid atherosclerotic plaques compared with healthy vessels. Strongly positive IHC staining of CXCR4 was detected in macrophages and macrophage-derived foam cells; nevertheless, IHC staining for CXCL12 showed no positive cells.

CXCL14 is an immune cell migration regulator in the CXC chemokine family with similar structure to CXCL12 [8]. As a novel non-ELR (glutamic acid-leucine-arginine) chemokine, CXCL14 has a short NH₂-terminal ending with only two amino acids (Ser-Lys) before the first typical cysteine residue, while CXCL12 and many other CXC chemokine families have five or more residues in their NH₂-terminal region [9]. ELR-negative chemokines mainly play

Associate Editor Nicola Smart oversaw the review of this article.

Electronic supplementary material The online version of this article (<https://doi.org/10.1007/s12265-019-09915-z>) contains supplementary material, which is available to authorized users.

✉ Zitian Huo
huozitian@126.com

✉ Guoping Wang
wanggp@hust.edu.cn

¹ Institute of Pathology, Tongji Hospital, Tongji Medical College, Huazhong University of Science and Technology, 430030 Wuhan, People's Republic of China

² Department of Pathology, School of Basic Medicine, Tongji Medical College, Huazhong University of Science and Technology, 430030 Wuhan, People's Republic of China

a role in chemotaxis of lymphocytes. However, CXCL14 shows neither chemotaxis effect on unactivated nor activated T cells [10]. These characteristics separate CXCL14 from other CXC chemokines and indicate a potentially unique role of CXCL14 in atherosclerosis.

It has been reported that the mRNA expression level of CXCL14 was not detected in freshly isolated human peripheral blood mononuclear cells [11]. Meanwhile, after being stimulated by lipopolysaccharide (LPS), transcript expression level of CXCL14 was detected in B cells rather than T cells [11]. But, up to now, the expression, localization, and function of CXCL14 have been unclear in atherosclerosis.

Materials and Methods

Immunofluorescence and Immunohistochemistry

The atherosclerosis tissues ($n = 28$) were obtained from surgically resected specimens. Specimens were retrieved using whole-tissue section, with informed consent being obtained from archival sources at the Tongji Hospital. Tissue sections were de-paraffinized and hydrated, and the endogenous peroxidase was blocked. Antigen retrieval was performed using the Dako Target Retrieval Solution, High PH (Dako Ominis, Agilent Technologies, Santa Clara, CA, USA), in a PTLINK set at 98 °C for 25 min. The tissue sections were incubated with an anti-CXCL14 rabbit polyclonal antibody, anti-CD163 rabbit monoclonal antibody (1:500) (Abcam, ab182422, USA), and anti-CD68 rabbit polyclonal antibody (1:100) (Abcam, ab125212, USA) overnight at 4 °C. Detection of immunostaining was achieved by an enzyme-conjugated polymer complex (K8002, Dako, Denmark) adapted for autostainers from DAKO (Dako Autostainer, Agilent Technologies). For immunofluorescence, the sample was prepared as previously mentioned, and mouse anti-CD68 antibody [KP1] (Abcam, ab955, USA) and rabbit anti-CXCL14 antibody (Abcam, ab46010, USA) were used for double staining overnight at 4 °C. Alexa-Fluor 488- or Alexa-Fluor 594-conjugated secondary antibodies were used for 1 h at room temperature. The nuclei were visualized by DAPI labelling. The images were acquired using Nikon fluorescence microscopy. The quantity of foam cells/macrophages that express CXCL14 was then assessed.

Cell Preparation and Culture

THP-1 cells were purchased from Fenghui Biology Company, and cell line authentication by STR (short-tandem repeat) was conducted by Shanghai Biowing Applied Biotechnology Co., Ltd. HPASMCs were purchased from Shanghai Xinyu

Biotechnology Co., Ltd. The cells were plated in Roswell Park Memorial Institute (RPMI) 1640 medium (HyClone, USA) with 10% fetal bovine serum (BIOIND, Israel) in CO₂ at 37 °C. THP-1 cells (1×10^6 /mL) were induced to differentiate into macrophages using 100 ng/mL PMA (Solarbio, China) for 24 h. Then, one group of the macrophages was washed and cultured with new media for another 24 h before cell lysis. The other group of macrophages was induced by 100 µg/mL ox-LDL (Yiyuan Biotech, China) for 24 h to differentiate into foam cells.

Preparation of Mouse Primary Macrophages

C57BL/6J mice were used to isolate primary peritoneal macrophage. After 3 days consecutive injection of 2 mL 4% thioglycollate, peritoneal macrophages were collected from the mice peritoneal cavity by infusing with 5 mL pre-cooled 1640 medium. Collected macrophages were centrifuged and washed with 1640 medium for two times and then cultured in Roswell Park Memorial Institute (RPMI) 1640 medium. Then, the primary peritoneal macrophages were cultured in 12-well plate for 6 h in an incubator with 5% CO₂ at 37 °C. The macrophages were treated with ox-LDL to induce foam cells after washing with PBS. The THP-1 cells or SMCs with neither CXCL14 nor fr180204 and the mouse primary macrophages with neither ox-LDL nor SP00125 served as negative control (NC).

Dual Luciferase Reporter Assay

We amplified oligonucleotides containing target sequences of CXCL14 (WT or MUT) and cloned into pmirGLO plasmids. Different plasmids (pcDNA3.1-AP-1 or pcDNA3.1) and vector (pGL3_CXCL14_WT or pGL3_CXCL14_MUT) were co-transfected with HEK293T cells using Lipofectamine 2000 (Invitrogen 11668-019) for 24 h. After 24 h, the cells were harvested and lysed. The activity reported by luciferase was measured using a dual luciferase assay kit (Promega E1910) and a multi-label plate reader (PerkinElmer). A group transfected with pGL3_basic vector served as negative control (NC).

Reagents

Recombinant human CXCL14 (Abcam, AB50043, USA) or mice CXCL14 (Abcam, ab202778, USA) was used at a terminal concentration of 100 nM, and the ERK1/2 inhibitor, fr180204 (MedChemExpress, HY-12275, China), was used at a terminal concentration of 1 µM in the following experiments.

Transwell Assays

Cell migration in response to CXCL14 was tested using a 24-well Boyden chamber (Corning, USA, 8 μm) as described in brief; 400 μL serum-free medium with 100 nM recombinant CXCL14 (Abcam, ab202778, USA) was added to the bottom wells of the chemotactic chamber. A total of 5×10^4 cells were resuspended in 200 μL serum-free medium and dropped to the top wells. Then, 12 h later, the cells were collected from the bottom wells. After being suspended and blended, an equal volume (100 μL) of cells in the lower chamber was added into 96-well plate and counted by CCK8 assay. The experiments were repeated in triplicate.

Scratch-Wound Assay

HPASMCs were allowed to grow until about 100% confluence in 12-well plate. Then, 200 μL pipette tip was used to create wound in the cell surface. After incubation for 0 or 24 h in serum-free medium at different conditions, the images were captured under microscope. The experiments were repeated in triplicate.

Cell Viability Analysis

SMA cells with different treatments were seeded at 2000 cells in 100 mL DMEM per well in 96-well culture plates. At the indicated time points, 100 mL of 10 $\mu\text{L}/\text{mL}$ Cell Counting Kit-8 (CCK-8; CK04–100, Dojindo, Kumamoto Prefecture, Kyushu, Japan) was added to each well and incubated at 37 $^{\circ}\text{C}$ for 3 h. The absorbance values (OD 450 nm) were measured using a multi-mode microplate reader (BioTek Synergy H1).

Western Blot

Cells were lysed in RIPA lysis buffer (R0278, Sigma-Aldrich, St. Louis, MO, USA) supplemented with phosphatase inhibitor cocktail tablets (04906845001, Roche) and protease inhibitor cocktail tablets (04693132001, Roche). Protein concentration was determined by the Enhanced BCA Protein Assay Kit (Thermo Fisher Scientific, USA), and gels were loaded with equal amounts of protein per lane. Electrophoretic separation was carried out on 10% polyacrylamide gels and subsequently transferred to NC membrane. Membranes were blocked in 5% BSA in TBST buffer for 1 h. Then, the membranes were incubated overnight at 4 $^{\circ}\text{C}$ with the following primary antibodies: rabbit anti-CXCL14 polyclonal antibody (1:3000) (Abcam, ab46010, USA), rabbit anti-c-Fos polyclonal antibody (1:1000) (CST, 4384, USA), rabbit anti-c-Jun monoclonal antibody (1:1000) (CST, 9165, USA), phospho-JNK rabbit monoclonal antibody (1:1000) (CST, 4668, USA), rabbit anti-JNK polyclonal antibody (1:1000) (CST, 9252, USA), rabbit anti-ERK1 + ERK2

polyclonal antibody (1:1000) (Abcam, ab17942, USA), phospho-p44/42 MAPK (Erk1/2) (Thr202/Tyr204), and rabbit monoclonal antibody (1:1000) (CST, 9101, USA), followed by incubation in the following secondary antibodies: HRP-goat anti-rabbit IgG (H + L) (1:2000) (Proteintech, China) or HRP-goat anti-mouse IgG (H + L) (1:2000) (Proteintech, China). Anti-beta-actin antibody (1:2500) (Abcam, ab8226, USA) and anti-GAPDH antibody (1:2000) (Santa Cruz, 0411, USA) served as the loading control in different experiments. The immunoblots were visualized with the SuperSignal West Femto Maximum Sensitivity Substrate (34,095, Thermo Fisher Scientific, Waltham, MA, USA).

RNA Isolation and qRT-PCR

Total RNA was prepared using TRIzol reagent (Invitrogen) and reverse-transcribed into cDNA by RevertAid cDNA Synthesis Kit (RR047A, Takara, Tokyo, Japan). PCR amplification was conducted on an ABI Prism 7900HT platform (Applied Biosystems, Foster City, CA, USA) using SYBR Green PCR Master Mix (04913850001, Roche, Basel, Switzerland). GAPDH was chosen as endogenous control. Relative quantification was assessed by the $2^{-\Delta\Delta\text{Ct}}$ method. The sequences of primers used are listed in Table 1.

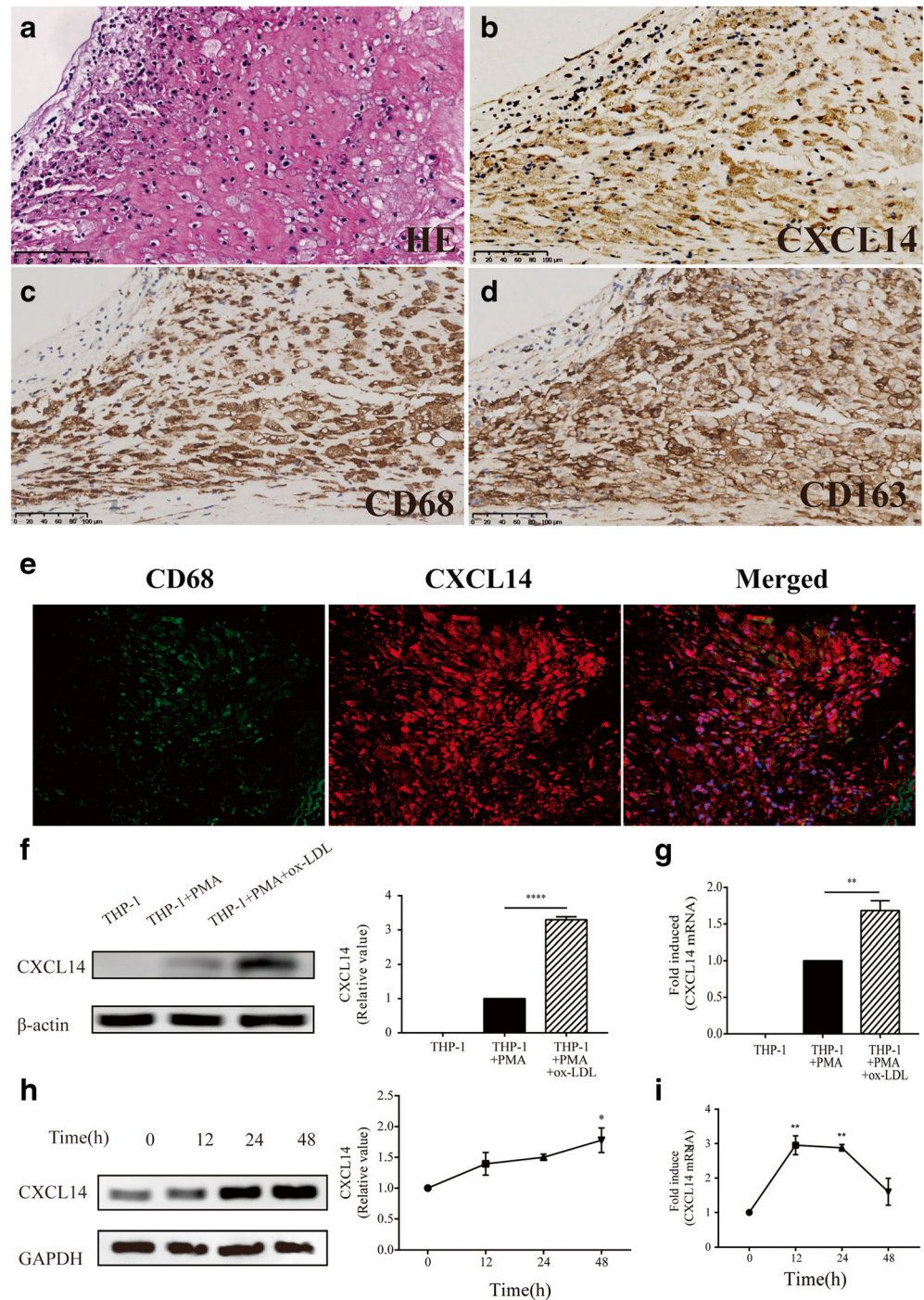
Oil Red O Staining

Induced macrophages were plated in 24-well plates for 24 h, and, then, one group of the macrophages was washed and cultured with new media for another 24 h before cell analysis. Other groups of macrophages were induced by 100 $\mu\text{g}/\text{mL}$ ox-LDL with or without CXCL14 (100 nM) for 24 h. The

Table 1 The sequences of primers for qRT-PCR

Gene	Primer sequence
Human CXCL14	
Forward	5'-CCCAAGCTGCAGAGCACC-3'
Reverse	5'-TAGACCCTGCGCTTCTCGTT-3'
Mouse CXCL14	
Forward	5'-GAAGATGGTTATCGTCACCACC-3'
Reverse	5'-CGTTCCAGGCATTGTACCACT-3'
c-Fos	
Forward	5'-CGGGTTTCAACGCCGACTA-3'
Reverse	5'-TTGGCACTAGAGACGGACAGA-3'
c-Jun	
Forward	5'-CCTTCTACGACGATGCCCTC-3'
Reverse	5'-GGTTCAAGGTCATGCTCTGTTT-3'
GAPDH	
Forward	5'-ACCCACTCCTCCACCTTTGA-3'
Reverse	5'-CATACCAGGAAATGAGCTTGACAA-3'

Fig. 1 CXCL14 was detected in macrophage-derived foam cell and up-regulated during foam cell formation. **(a)** HE staining of the atheromatous plaques. **(b)** Typical positive IHC staining of CXCL14. **(c–d)** IHC staining of CD68 and CD163. **(e)** Immunofluorescence double staining of CD68 and CXCL14. Western blot **(f)** and real-time PCR **(g)** analysis of CXCL14 in THP-1 cells in different stages during foam cell formation. Western blot **(h)** and real-time PCR **(i)** demonstrated that ox-LDL promoted CXCL14 expression in mouse primary macrophages. Data are expressed as the mean \pm SEM ($n = 3$). $*p < 0.05$



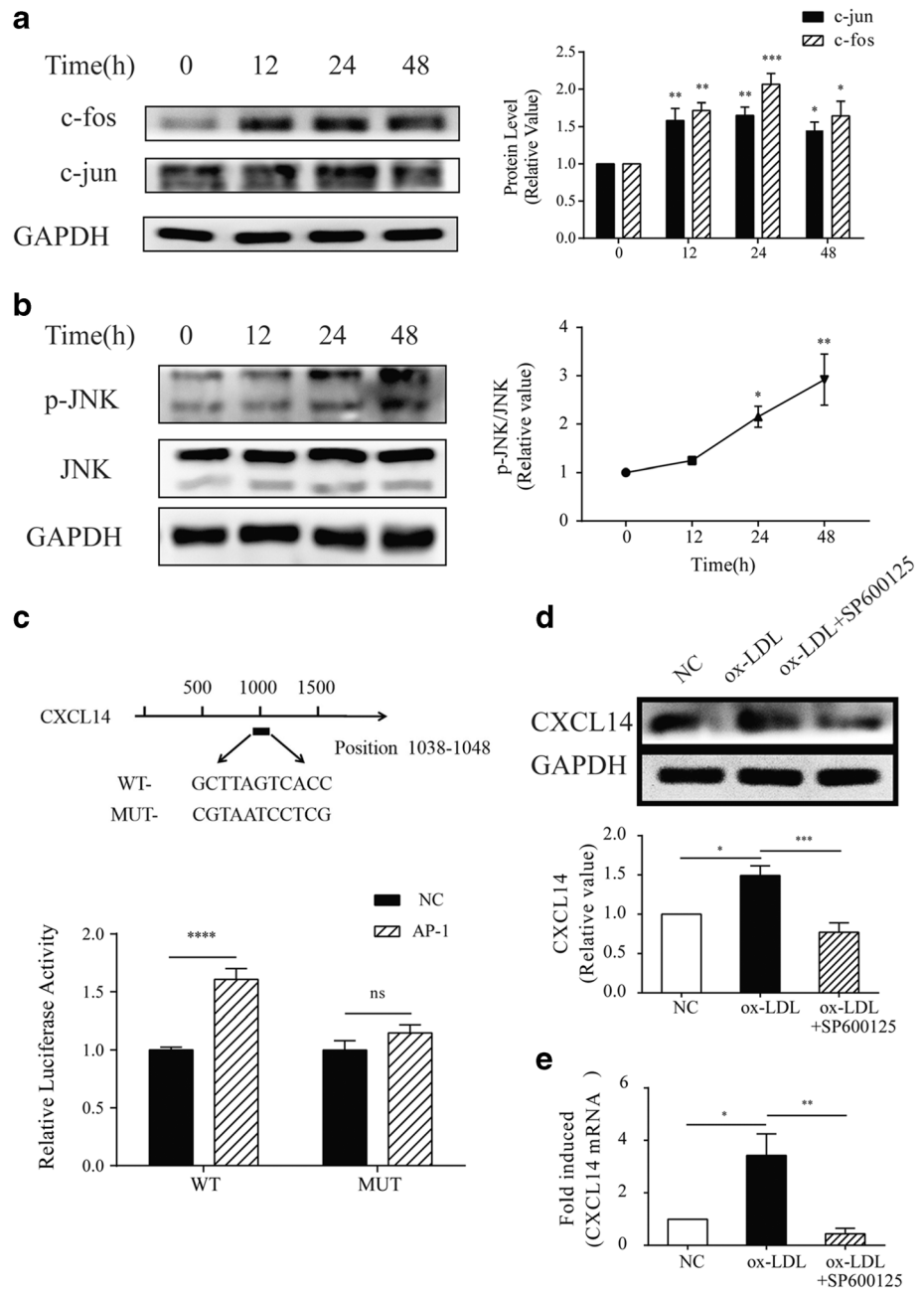
cells were washed twice with PBS, fixed with 10% formaldehyde overnight at 4 °C, and washed twice with PBS. Then, the cells were washed with 60% isopropyl alcohol once before staining. The cells were stained for 15 min at room temperature in freshly diluted Oil Red O Solution (stock solution, 0.5 g Oil Red O powder dissolved in 100 mL isopropanol, then heated in a 65 °C water bath for 30 min, cooled, and filtered with a 0.22 μ m filter), and then washed twice with distilled water. The cells were observed using an inverted microscope.

For quantification, the stained cells were eluted with isopropyl alcohol for 5 min, and the OD value was determined at 510 nm subsequently.

Experiment Mouse Model, CXCL14 Peptide, and Lesion Analyses

Eight-week-old male ApoE^{-/-} mice on the C57BL/6 background were obtained from GemPharmatech Co., Ltd. (catalog #T001458). CXCL14 peptide was produced by

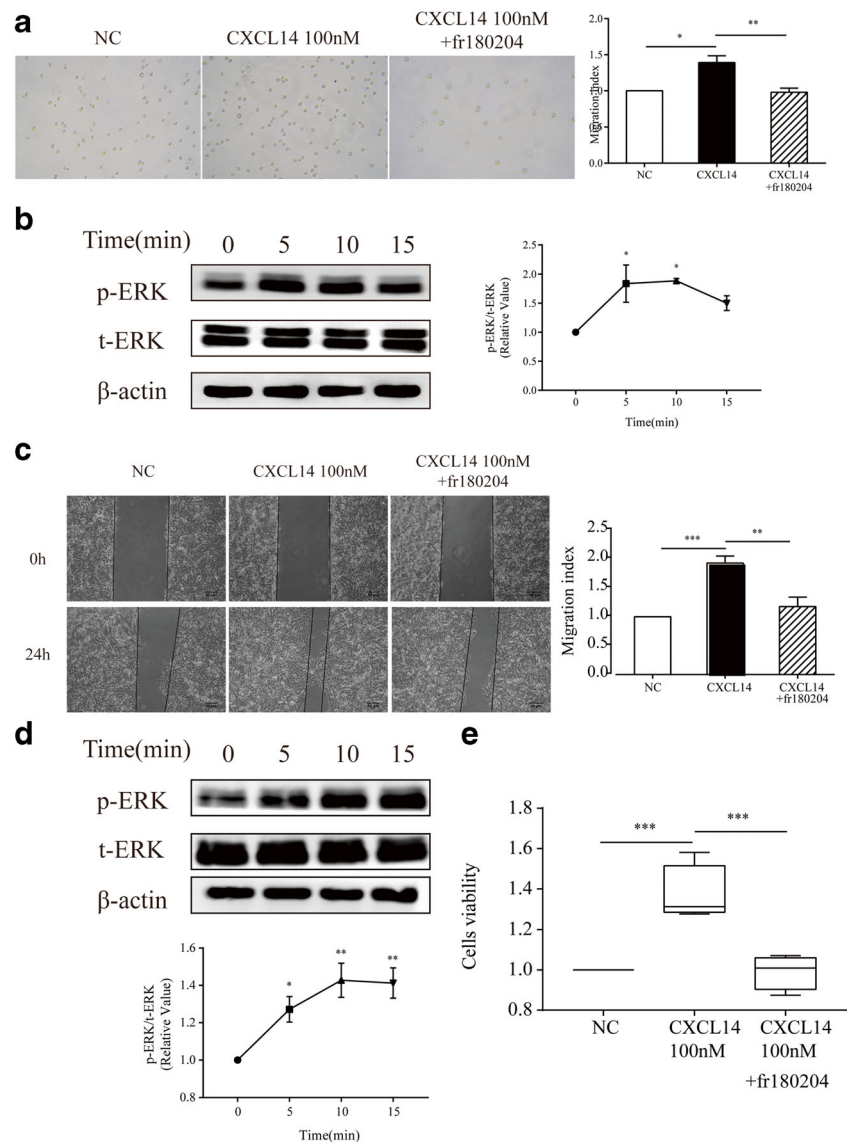
Fig. 2 ox-LDL promoted CXCL14 expression via AP-1/JNK pathway in vitro. **(a)** c-Jun and c-Fos (two subunits of AP-1) increased in ox-LDL-induced mouse primary macrophages. **(b)** ox-LDL-induced JNK phosphorylation in mouse primary macrophages. **(c)** Dual luciferase reporter assay demonstrated that AP-1 could bind to CXCL14 promoter and up-regulate CXCL14 mRNA expression. NC refers to a negative control group transfected with pGL3_basic vector. In vitro, SP600125 (inhibitor of JNK pathway) reversed ox-LDL induced up-regulation of CXCL14 at both protein **(d)** and mRNA levels **(e)**. NC represents mouse primary macrophages with neither ox-LDL nor SP00125. Data are expressed as the mean \pm SEM ($n = 3$). * $p < 0.05$



Bioyaregene Biosciences Co., Ltd.; peptide 1: 51-71CEEKMVIVTTKSMRSRYRGQEH and peptide 2: 27-40CSRKGPKIRYSDVK. ApoE^{-/-} mice at 8 weeks of age were fed a normal diet as negative control group (NC) or western diet (WD, 40% fat/0.15% cholesterol) for 3 months, and those treated with WD were given NS (normal saline) as placebo group, scramble peptide (GHQTTKVIESREKVRM) as scramble group, or CXCL14 peptide injections. We IH injected 15 mg/kg CXCL14 peptide once every three weeks to keep appropriate serum antibody levels. The peptides were injected subcutaneously. Two different designed CXCL14 peptides were used as two experiment groups; information was the same as that described previously. At specific time

points, ApoE^{-/-} mice treated with their respective dietary regimens and treated with or without CXCL14 anti-peptide were sacrificed and perfused with isotonic EDTA-PBS solution after venous blood collection. This was followed by in situ fixation at physiological pressure with formal sucrose (4% paraformaldehyde). Aortas were then dissected, opened longitudinally, and stained with Oil Red O. The aorta was pressed onto a slide and covered with a coverslip (after removal of the adventitia), the image was scanned, and the percentage of atherosclerotic surface area was determined by computer-assisted image analysis. At sacrifice, the heart and proximal aorta were obtained and embedded in optimal cutting temperature compound. Aortic root cross-sectional atherosclerosis

Fig. 3 CXCL14 promoted THP-1 and SMC migration via ERK1/2 pathway in vitro. **(a)** Transwell assay showed that CXCL14 promoted THP-1 cell migration and the chemotaxis effect of CXCL14 could be blocked by fr180204 (ERK1/2 inhibitor). NC represents THP-1 with neither CXCL14 nor fr180204. **(b)** CXCL14 induced ERK1/2 phosphorylation in THP-1 cells. **(c)** Wound-healing assay showed that CXCL14 promoted SMCs migration, of which effect could be blocked by fr180204. **(d)** CXCL14 induced ERK1/2 phosphorylation in SMCs. **(e)** CCK8 assay showed that CXCL14 promoted SMC proliferation in vitro, which could also be blocked by fr180204. NC represents SMCs with neither CXCL14 nor fr180204. Data are expressed as the mean \pm SEM ($n = 3$). $*p < 0.05$



was measured by cutting sections through the whole proximal aorta. Quantitative analysis of lesion and necrotic area was performed on each section with about 10 sections analyzed, spanning 1000 μ m from the origin of the first visible leaflet. The results are presented as total lesion or necrotic area in mm^2 of all aortic cross-sections analyzed.

Statistical Analysis

All data are represented as the mean \pm SEM. Statistical analyses were performed using GraphPad Prism 7 (GraphPad Software, La Jolla, CA, USA). Data were analyzed using a one-way analysis of variance (ANOVA) followed by Tukey's honestly significant difference test. $P < 0.05$ was considered statistically significant.

Results

CXCL14 Was Expressed in Foam Cells Both in Atherosclerosis Specimens and Macrophage-Derived Foam Cells In Vitro

Immunohistochemistry detected positive CXCL14 staining in the surgically resected specimens of patients suffering atherosclerosis. The positive cytoplasm staining could be seen in all samples regardless of age, sex, or lesion locations (Table 2). Given the hematoxylin and eosin (HE) staining images as well as the positive immunohistochemical staining of CD163 and CD68, it is noteworthy that CXCL14 was localized mainly at macrophage-derived foam cells (Fig. 1a–d). In addition, double immunofluorescence staining of CXCL14 and CD68 showed that nearly 100% foam cells/macrophage expressed CXCL14 (Fig. 1e).

Table 2 Patient characteristics

Characteristic	No. of patients (%)
Total	28
Gender	
Male	24 (85.71%)
Female	4 (14.29%)
Age	59.96 (39–78)
60 ≥	15 (53.57%)
60 <	13 (46.43%)
Neurological symptoms	15 (53.57%)
Hypertension	18 (64.29%)
Diabetes mellitus	2 (7.14%)
Smoking	10 (35.71%)
Chronic kidney disease	3 (10.71%)
Coronary disease	4 (14.29%)
Peripheral artery disease	10 (35.71%)
Medical treatment	
Aspirin/Clopidogrel	14 (50%)
Beta-blocker	9 (32.14%)
ACE I	6 (21.43%)
Statins	14 (50%)
Diuretics	10 (35.71%)

In vitro, THP-1 cells with suspension growth characteristics were adherent as macrophages after being treated with 100 ng/mL PMA for 24 h. The formation of macrophage-derived foam cells was realized by an additionally followed treatment of 100 μg/mL ox-LDL for another 24 h. Western blot assay and real-time PCR results showed that CXCL14 was not expressed in quiescent THP-1 cells but THP-1-derived foam cells expressed CXCL14 remarkably (Fig. 1f, g). In addition, 100 μg/mL ox-LDL was added to cultured mouse primary macrophages. Over time, CXCL14 is also up-regulated both at protein and mRNA levels (Fig. 1h, i).

Ox-LDL Induced CXCL14 Expression Via AP1 Pathway in Mouse Primary Macrophages

We explored the molecular mechanisms on how ox-LDL up-regulated CXCL14 expression in cultured mouse primary macrophages. We use two different approaches to survey an ox-LDL-activated pathway AP-1. Firstly, we examined the expression of two subunits of the AP-1 complex (c-Jun and c-Fos) after adding 100 μg/mL ox-LDL to mouse primary macrophages for 0, 12, 24, and 48 h. Over time, both c-Jun and c-Fos were elevated and peaked at 24 h (Fig. 2a). On the other hand, we examined the phosphorylation activity of c-Jun-NH2-kinase (JNK) under ox-LDL stimulation. Noteworthy, there was no

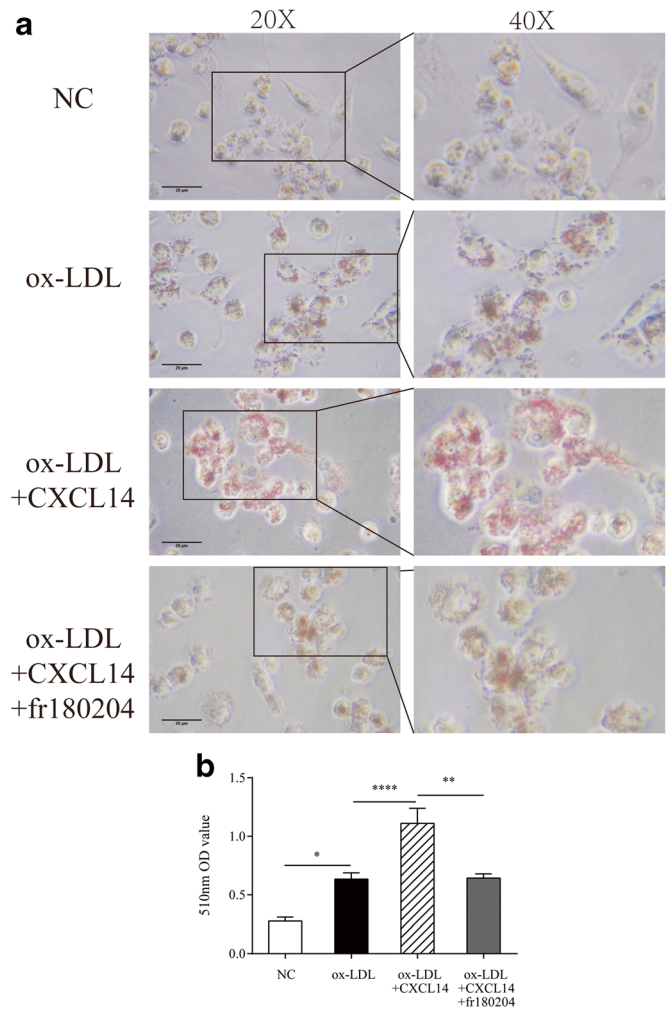
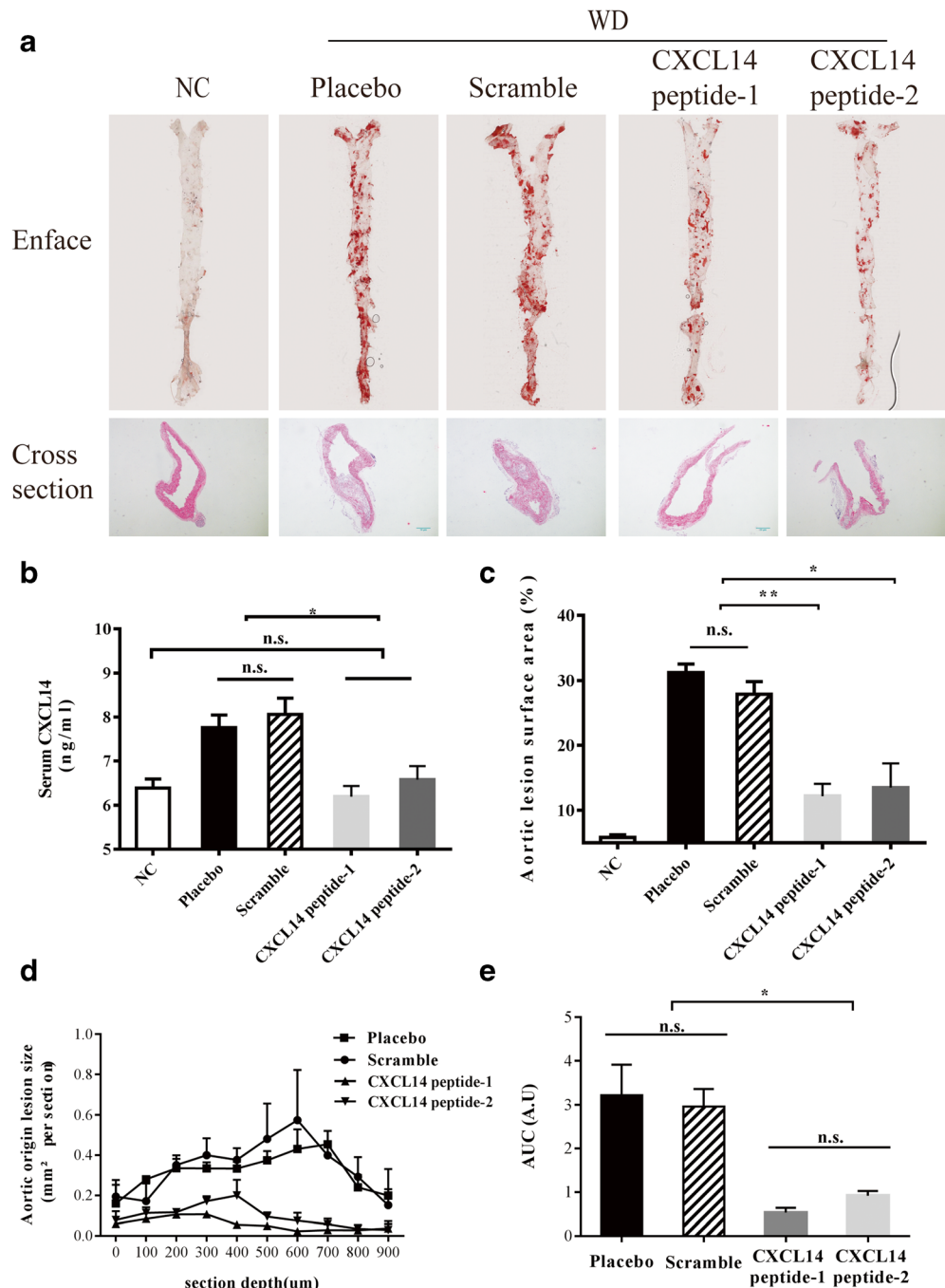


Fig. 4 CXCL14 promoted lipid phagocytosis via ERK1/2 pathway in vitro. (a) Oil Red O staining assay showed that CXCL14 promoted THP-1-derived macrophage lipid phagocytosis, which could be reversed by fr180204. (b) Statistical semi-quantitative processing by 510 nm OD value. NC refers to macrophages (induced by PMA) with neither ox-LDL nor CXCL14 and fr180204. Data are expressed as the mean ± SEM (n = 3). *p < 0.05

change in total JNK protein in the presence of ox-LDL, while ox-LDL induced approximately 3-fold higher JNK phosphorylation compared to the control group (Fig. 2b). In addition, the results of the dual luciferase reporter gene also showed that AP1 could directly bind to and activate the CXCL14 promoter (Fig. 2c). To further confirm the involvement of JNK in this process, macrophages were treated with the JNK inhibitor SP600125 to block c-Jun activation. After culturing in the new medium in the presence of ox-LDL for another 24 h, the macrophages were harvested and detected CXCL14 expression at the protein and mRNA levels (Fig. 2d, e). These results showed that the JNK inhibitor indeed attenuated the promotion of ox-LDL-induced CXCL14 expression.

Fig. 5 CXCL14 peptide immunotherapy reduced atherosclerotic lesions in ApoE^{-/-} mouse atherosclerosis model. **(a)** Typical Oil Red O staining of enface total aorta and HE staining of cross-section. **(b)** Serum CXCL14 levels were detected by ELISA. CXCL14 peptide immunotherapy reduced serum CXCL14 compared with placebo or scramble group. Aortic lesion surface area **(c)**, cross-sectional aortic root analyses of lesion size **(d)**, and area-under-the-curve (AUC) **(e)** analyses demonstrated therapeutic value of CXCL14 peptide immunotherapy. NC refers to the group which was fed a normal diet. Data are expressed as the mean \pm SEM ($n = 3$). * $p < 0.05$



CXCL14 Promotes THP-1 Cell Migration, Vessel Smooth Muscle Cell Migration, and Proliferation Via ERK1/2 Pathway

Transwell assay suggested that CXCL14 had chemotaxis effect on THP-1 cells (Fig. 3a). The scratch-wound assay was applied to investigate the migration effect of CXCL14 in HPASMCs (Fig. 3c). Besides, when stimulated by 100 nM recombinant CXCL14, the phosphorylation level of ERK1/2 was up-regulated in THP-1 cells (Fig. 3b) and HPASMCs (Fig. 3d). When inhibiting the

ERK1/2 pathway with fr180204 (a competitive inhibitor), the chemotaxis effect on THP-1 cells and smooth muscle cells could be blocked. CXCL14 also promoted smooth muscle cell proliferation, and this effect could also be blocked by ERK1/2 inhibitor (Fig. 3e).

CXCL14 Promoted Macrophage Lipid Phagocytosis Via ERK1/2 Pathway

Oil Red staining and quantification were used to investigate the phagocytosis of lipids in macrophages, which

were derived from THP-1 cells by 100 ng/mL PMA. Similarly, the results showed that the group with 100 ng/mL recombinant CXCL14 could phagocytose more lipids than the control group. The promotion effect on macrophage lipid phagocytosis was attenuated by the ERK1/2 inhibitor, fr180204 (Fig. 4a, b).

CXCL14 Peptide Immunotherapy Reduced Atherosclerotic Lesions in ApoE^{-/-} Mouse Atherosclerosis Model

Typical enface and cross-section images of each group were shown in Fig. 5a. At sacrifice, total serum CXCL14 levels in the CXCL14 peptide groups were significantly lower compared with placebo or scramble group mice (Fig. 5b), while there was no change in body weight (data not shown). We determined the percentage of aorta's atherosclerotic surface area by computer-assisted image analysis. CXCL14 peptide treatment noticeably reduced enface aortic lesion area by 50% (Fig. 5c). Analysis of serial sections of the aortic root demonstrated comparable 70% decreases in lesion area within the lesions in CXCL14 peptide-treated ApoE^{-/-} mice compared to placebo or scramble groups (Fig. 5d, e).

Discussion

Many normal tissues, such as breast and kidney [12], constitutively express CXCL14 at high level, while it is reduced or absent in most cancer cells, including head-and-neck carcinoma, lung adenocarcinoma, and prostate cancer [13–15]. CXCL14 was very early reported to target tissue macrophages, promote white adipose tissue macrophage migration, and regulate glucose metabolism mainly in the skeletal muscle [16]. Several previous studies [17, 18] have also noticed that CXCL14 was not expressed in THP-1 cells; however, the relationship between CXCL14 and atherosclerosis has been rarely investigated.

In this study, strong CXCL14 expression was detected at foam cells in atherosclerosis plaque by IHC. We further confirmed the absence of CXCL14 in THP-1 cells and observed up-regulation of CXCL14 in both THP-1 and primary isolated mice macrophages under ox-LDL treatment. Generally, oxidative stress could affect the expression of CXCL14 through the AP-1 pathway [19]. Similarly, ox-LDL has been shown to induce AP-1 and NF- κ B signaling in endothelial cell [20, 21]. In atherogenesis, monocytes are recruited to plaque and transform into foam cells when stimulated by ox-LDL. In the THP-1-derived foam cell model, our results suggested that AP-1 is activated by ox-LDL stimulation and its inhibitors attenuate CXCL14 expression induced by ox-LDL. Through dual-luciferase reporter assay, it was demonstrated that AP-1 binds to CXCL14 promoter and up-regulates CXCL14 mRNA expression, which could explain how ox-LDL affects CXCL14 expression in atherosclerosis.

Monocyte and smooth muscle cell migration towards plaque, smooth muscle proliferation in plaque, and macrophage lipid phagocytosis are three critical processes in atherogenesis and development of atherosclerosis. In this study, it was indicated that CXCL14 paracrine functions as one ring of the positive feedback loop of monocyte recruitment. Interestingly, we also noticed that CXCL14 autocrinely promotes lipid phagocytosis. Besides, CXCL14 could paracrine promote vessel smooth muscle cell migration and proliferation too. These atherosclerotic effects of CXCL14 suggest it to be a possible therapeutic target in atherosclerosis treatment.

Vaccination against peptides specific to Alzheimer's disease (such as amyloid- β or tau) may generate an immune response that could help inhibit disease and symptom progression [22]. As the receptor of CXCL14 remains unknown, we put forward a similar peptide-based immune interventional method to inhibit CXCL14 function in ApoE^{-/-} mice model. As a result, CXCL14 peptide immunotherapy successfully reduced serum CXCL14 protein levels compared with placebo or scramble group, and distinct therapeutic value was observed.

In conclusion, CXCL14 is highly up-regulated during foam cell formation and plays an atherosclerotic role in various ways. Vaccination against specific CXCL14 peptides could be an effective therapy for atherosclerosis treatment.

Author Contributions W.T., R.Y., C.P., and Y.W. conducted the experiments. Y.D. analyzed the results. W.T. wrote the manuscript. Z.H. and G.W. conceived the experiments. All authors reviewed the manuscript.

Funding Information This study was supported in part by research grants 81770263, 81570254, and 31271040 from the National Natural Science Foundation of China.

Compliance with Ethical Standards

All experimental protocols were approved by the Ethical Committee of Tongji Hospital, Tongji Medical College, Huazhong University of Science and Technology. All animal studies were performed in accordance with the Guidelines of the Hubei Council of Animal Care and approved by the Experimental Animal Committee of the Huazhong University of Science and Technology in China. The informed consent was obtained from all subjects, and this study is approved by the Ethical Committee of Tongji Hospital, Tongji Medical College, Huazhong University of Science and Technology.

Competing Interests The authors declare that they have no competing interests.

References

1. Ference, B. A., Ginsberg, H. N., Graham, I., et al. (2017). Low-density lipoproteins cause atherosclerotic cardiovascular disease. 1. Evidence from genetic, epidemiologic, and clinical studies. A

- consensus statement from the European Atherosclerosis Society Consensus Panel.[J]. *European Heart Journal*, 38, 2459–2472.
2. Cao Dian, J. (2018). Macrophages in cardiovascular homeostasis and disease.[J]. *Circulation*, 138, 2452–2455.
 3. Tabas, I., & Lichtman, A. H. (2017). Monocyte-macrophages and T cells in atherosclerosis.[J]. *Immunity*, 47, 621–634.
 4. Puca, A. A., Carrizzo, A., Spinelli, C., et al. (2019). Single systemic transfer of a human gene associated with exceptional longevity halts the progression of atherosclerosis and inflammation in ApoE knockout mice through a CXCR4-mediated mechanism.[J]. *European Heart Journal* published ahead of time.
 5. Li, X., Kemmer, L., Zhang, X., et al. (2018). Anti-inflammatory effects on atherosclerotic lesions induced by CXCR4-directed endoradiotherapy.[J]. *Journal of the American College of Cardiology*, 72, 122–123.
 6. Sainz, J., & Sata, M. (2007). CXCR4, a key modulator of vascular progenitor cells.[J]. *Arteriosclerosis, Thrombosis, and Vascular Biology*, 27, 263–265.
 7. Merckelbach, S., van der Vorst, E. P. C., Kallmayer, M., et al. (2018). Expression and cellular localization of CXCR4 and CXCL12 in human carotid atherosclerotic plaques.[J]. *Thrombosis and Haemostasis*, 118, 195–206.
 8. Salogni, L., Musso, T., Bosisio, D., et al. Activin A induces dendritic cell migration through the polarized release of CXC chemokine ligands 12 and 14. *Blood*, 113(23), 5848–5856.
 9. Lu, J., Chatterjee, M., Schmid, H., et al. CXCL14 as an emerging immune and inflammatory modulator. *Journal of Inflammation (Lond)*, 13, 1.
 10. Sleeman, M. A., Fraser, J. K., Murison, J. G., Kelly, S. L., et al. B cell- and monocyte-activating chemokine (BMAC), a novel non-ELR alphachemokine. *International Immunology*, 12(5), 677–689.
 11. Frederick, M. J., Henderson, Y., et al. In vivo expression of the novel CXC chemokine BRAK in normal and cancerous human tissue. *The American Journal of Pathology*, 156(6), 1937–1950.
 12. Kurth, I., Willmann, K., Schaerli, P., et al. Monocyte selectivity and tissue localization suggests a role for breast and kidney-expressed chemokine (BRAK) in macrophage development. *The Journal of Experimental Medicine*, 194(6), 855–861.
 13. Ozawa, S., Kato, Y., Komori, R., et al. BRAK/CXCL14 expression suppresses tumor growth in vivo in human oral carcinoma cells. *Biochemical and Biophysical Research Communications*, 348(2), 406–412.
 14. Tessema, M., Klinge, D. M., Yingling, C. M., et al. Re-expression of CXCL14, a common target for epigenetic silencing in lung cancer, induces tumor necrosis. *Oncogene*, 29(37), 5159–5170.
 15. Song, E. Y., Shurin, M. R., Tourkova, I. L., et al. Epigenetic mechanisms of promigratory chemokine CXCL14 regulation in human prostate cancer cells. *Cancer Research*, 70(11), 4394–4401.
 16. Nara, N., Nakayama, Y., Okamoto, S., et al. (2007). Disruption of CXC motif chemokine ligand-14 in mice ameliorates obesity-induced insulin resistance.[J]. *The Journal of Biological Chemistry*, 282, 30794–30803.
 17. Tanegashima, K., Suzuki, K., Nakayama, Y., et al. (2010). Antibody-assisted enhancement of biological activities of CXCL14 in human monocytic leukemia-derived THP-1 cells and high fat diet-induced obese mice.[J]. *Experimental Cell Research*, 316, 1263–1270.
 18. Poon, W.-L., Alenius, H., Ndika, J., et al. (2017). Nano-sized zinc oxide and silver, but not titanium dioxide, induce innate and adaptive immunity and antiviral response in differentiated THP-1 cells.[J]. *Nanotoxicology*, 11, 936–951.
 19. Pelicano, H., et al. Mitochondrial dysfunction and reactive oxygen species imbalance promote breast cancer cell motility through a CXCL14-mediated mechanism. *Cancer Research*, 69(6), 2375–2383.
 20. Foncea, R., Mazière, C., et al. Endothelial cell oxidative stress and signal transduction. *Biological Research*, 33(2), 89–96.
 21. Suxia, M., Zhifeng, B., et al. The DPP-4 inhibitor saxagliptin ameliorates ox-LDL-induced endothelial dysfunction by regulating AP-1 and NF- κ B. *European Journal of Pharmacology*, 851, 186–193.
 22. Sterner, R. M., Takahashi, P. Y., Yu, B., & Aimee, C. (2016). Active vaccines for Alzheimer disease treatment.[J]. *Journal of the American Medical Directors Association*, 17, 862.e11–862.e15.

Publisher's Note Springer Nature remains neutral with regard to jurisdictional claims in published maps and institutional affiliations.